Galaxy Evolution and Feedback across Different Environments
Proceedings IAU Symposium No. 359, 2020
T. Storchi-Bergmann, W. Forman, R. Overzier & R. Riffel, eds.
doi:10.1017/S174392132000174X

The light side of proto-cluster galaxies at $z \sim 4$

Kei Ito

Department of Astronomical Science, The Graduate University for Advanced Studies, SOKENDAI, Mitaka, Tokyo, 181-8588, Japan
email: kei.ito@grad.nao.ac.jp

Abstract. Overdense regions at high redshift, which are often called "protoclusters", are thought to be a place where the early active structure formations are in progress. Thanks to the wide and deep-sky survey of Hyper Suprime-Cam Subaru Strategic Program, we have selected 179 protocluster candidates at $z \sim 4$, enabling us to statistically discuss high-z overdense regions. I report results of the HSC-SSP protocluster project, focusing on a couple of results on the bright-end of protocluster galaxies. We identify the UV-brightest galaxies, which are likely progenitors of Brightest Cluster Galaxies. We find that these are dustier and larger than field galaxies. This suggests that galaxies in protoclusters have experienced different star formation histories at $z \sim 4$. Also, the UV luminosity function of galaxies in protoclusters (PC UVLF) has a significant excess on the bright-end from field UVLF. The PC UVLF suggests that protoclusters contribute $\sim$5−16% of the total cosmic SFRD at $z \sim 4$. The result implies that early galaxy formation occurs in protoclusters.

Keywords. galaxies: evolution, galaxies: clusters: general, galaxies: high-redshift

1. Introduction

Properties of galaxies in galaxy clusters are known to be different from those of galaxies in the field (e.g., Dressler 1980). Searching progenitors of these clusters at high redshift and investigating properties of their galaxies can give some clues for unveiling origins of such an effect of overdense regions. Therefore, overdense regions at high redshift, so-called protoclusters, which are defined as structures that will collapse into virialized objects with $\geqslant 10^{14} M_\odot$ at $z \geqslant 0$, are unique targets. These have been found through a large variety of selection techniques and various tracers at $z \sim 2-7$.

Observational studies show that protocluster galaxies at $z \sim 2$ have different properties compared to field galaxies at the same epoch. They tend to have enhancements of star formation rates (SFRs) (e.g., Shimakawa *et al.* 2018; Koyama *et al.* 2013), with larger stellar mass (above references and Cooke *et al.* 2014; Hatch *et al.* 2011; Steidel *et al.* 2005). Several theoretical simulations support these trends and suggest that galaxies in protoclusters experience earlier formation and are a significant contribution to the cosmic star formation rate density (SFRD) at $z \geqslant 2$ (e.g., Chiang *et al.* 2017; Lovell *et al.* 2018; Muldrew *et al.* 2015). Extending the study of protocluster galaxies properties is essential to understand the origin of the environmental effect. However, due to the low number density of protocluters and the various techniques to detect them, they had not yet been systematically investigated at $z > 3$.

Recently, we have conducted a new protocluster survey from the photometric data of the Hyper Suprime-Cam (HSC) Subaru Strategic Program (HSC-SSP) (Aihara *et al.* 2018). Our protocluster survey is based on Lyman break galaxies (LBGs), and we have already selected 179 protocluster candidates from g-dropout galaxies over an area of 121 deg^2 (Toshikawa *et al.* 2018). Based on this sample, we have conducted several follow-up studies, investigating the relationship between overdensity and bright quasars in Uchiyama *et al.* (2018), and quasar pairs in Onoue *et al.* (2018), and using the stacked infrared (IR) properties of protoclusters to probe obscured star formation and active galactic nuclei in Kubo *et al.* (2019). Here, we report two results of rest-ultraviolet (rest-UV) bright galaxies in these protoclusters; the rest-UV properties of UV-brightest galaxies Ito *et al.* (2019) and the rest-UV luminosity function (UVLF) of protocluster galaxies (PC UVLF) (Ito *et al.* submitted). According to the star-formation main sequence, the UV-brightest galaxies are expected to be the most massive among other g-dropout members, which means that they can be progenitors of Brightest Cluster Galaxies in the local universe (hereafter proto-BCGs). Various papers have studied the UVLF of field galaxies, and they are the dominant diagnostics of the cosmic SFRD at $z \sim 3{-}8$. The PC UVLF enables us to estimate the contribution of protoclusters to the cosmic SFRD and examine whether protocluster galaxies have different properties, even at $z \sim 4$.

2. The UV-brightest Protocluster Galaxies

Since we are focusing on the significantly brightest galaxies compared to other protocluster members, we select the UV-brightest galaxies, which are 1 mag brighter than the fifth brightest galaxies in each protocluster in the rest-UV. As a result, we select 63 brightest protocluster galaxies from 179 protoclusters. For the detailed selection method, including the protocluster selection, see Ito *et al.* (2019).

We compare two properties; rest-UV color ($i{-}z$ for $z \sim 4$) and rest-UV size. When comparing the rest-UV color, we match the UV luminosity of reference field galaxies to that of proto-BCGs in order to exclude the effect of the relation of the brightness and color (e.g., Bouwens *et al.* (2009)) The left panel of Figure 1 shows the distribution of $i{-}z$ colors of proto-BCGs and field galaxies. We can see that the proto-BCGs are redder than field galaxies. The rest-UV color of galaxies is believed to be primarily related to their dust extinction. This suggests that proto-BCGs are dustier than field galaxies with the same luminosity.

Next, we estimate the average rest-UV size for proto-BCGs. We use i band images taken from HSC-SSP since it has the best image quality in terms of seeing and depth. For maximizing the signal to noise ratio, the images of all proto-BCGs were average-stacked. The average radial profile of the magnitude matched field galaxies sample is also derived in the same manner. The radial profile of proto-BCGs looks more extended than that of field galaxies. To quantitatively discuss this feature, we fit the 2D galaxy surface profile to stacked images by using `GALFIT`. We employ the Sérsic profile (Sérsic 1963) assuming the Sérsic index to be −1.5, following Shibuya *et al.* (2015). We plot our proto-BCGs value compared to the size-luminosity relation of field galaxies from Shibuya *et al.* (2015) in the right panel of Figure 1. The value of field galaxies estimate in this study is also overplotted, and they are consistent with Shibuya *et al.* (2015), suggesting that our estimation is in good agreement with previous studies. Proto-BCGs are 28% larger than field galaxies.

In this UV-brightest protocluster galaxy study, we find that UV-brightest galaxies in HSC-SSP protoclusters at $z \sim 4$ are dustier and have larger sizes in rest-UV. The result suggests that the environmental effect has occurred at $z \sim 4$, at least for the UV-brightest galaxies. The proper study for all protocluster members is crucial for understanding the whole picture of the environmental effect.

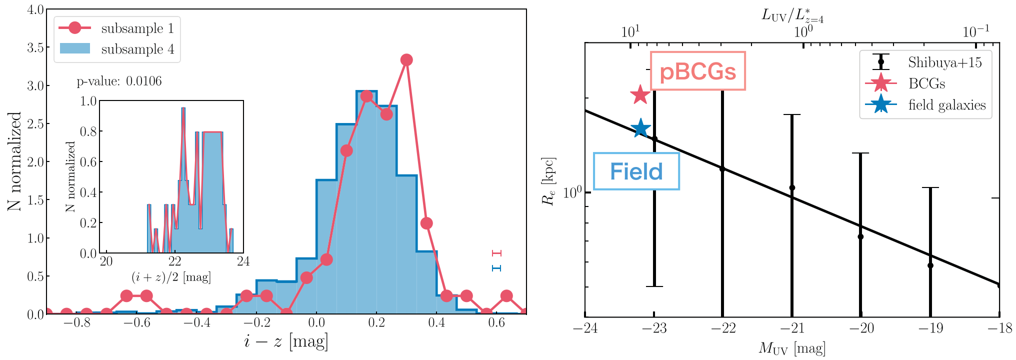

Figure 1. Left Panel: The $i-z$ color distribution of proto-BCGs (red line) and field galaxies (blue histogram) at the same brightness, edited from Ito *et al.* (2019). The typical UV magnitude ($(i+z)/2$) is shown in the inset. The result of the Anderson-Darling test suggests that the p-value $p=1.1\times10^{-2}$, so we reject the null hypothesis that these two color distributions are the same. Right Panel: The average size-luminosity relation of proto-BCGs (red star). A blue star is that of magnitude-matched field galaxies. Black dots correspond to a size-luminosity relation of LBGs at $z\sim4$ from Shibuya *et al.* (2015).

3. The rest-UV luminosity function of protocluster galaxies

We derive a UVLF of g-dropout galaxies in HSC-SSP protocluster at $z\sim4$. Here, we define protocluster galaxies as objects that are located within $1'.8$ from overdensity peak of each of the 179 protocluster. This size corresponds to the typical size of protoclusters predicted in theoretical simulations (Chiang *et al.* 2013).

Here, we describe the procedure for deriving the PC UVLF. We first derive the completeness function of our g-dropout galaxy sample and the UVLF of field galaxies. Then from the number count of protocluster members and these functions, we derive the PC UVLF $\Phi_{\rm PC}(M_{\rm UV})$ following this equation:

$$\Phi_{\rm PC}(M_{\rm UV})=\frac{1}{F(M_{\rm UV})}\left(\frac{n_{\rm obs,PC}(M_{\rm UV})}{V_{\rm eff}(M_{\rm UV})}-\Phi_{\rm field}(M_{\rm UV})\right) \qquad (3.1)$$

Here, $n_{\rm obs,PC}(M_{\rm UV})$ is the observed number of g-dropout galaxies in protocluster regions, $\Phi_{\rm field}(M_{\rm UV})$ is the luminosity function of field galaxies without the contamination correction, and $V_{\rm eff}(M_{\rm UV})$ is the effective volume of g-dropout galaxies derived from the completeness function. $F(M_{\rm UV})$ is the correction factor of the effective volume of protoclusters from the entire g-dropout galaxies since they are located in a significantly smaller volume than field galaxies. HSC-SSP protoclusters are located in 5 fields (GAMA15H, HECTOMAP, VVDS, WIDE12H, and XMM), and since the depth of each field can be different, we estimate PC UVLF for each field separately.

Figure 2 shows our PC UVLF. Two differences found for the PC UVLF can be seen from this figure. First, the amplitude of the PC UVLF is higher than that of field galaxies. This is because we focus on protoclusters, which are galaxy overdense regions. Secondly, also the shape of the PC UVLF is different from that of the field UVLF. We can see the PC UVLF has flatter shape than that of field galaxies. This implies that protocluster galaxies are brighter in the rest-UV than field galaxies. It is known that rest-UV light can be converted to the star formation rate (SFR) (Kennicut 1998), so brighter galaxies in protoclusters means higher SFRs for protocluster galaxies, which supports the existence of the environment effect on galaxy properties even at $z\sim4$.

https://doi.org/10.1017/S174392132000174X Published online by Cambridge University Press

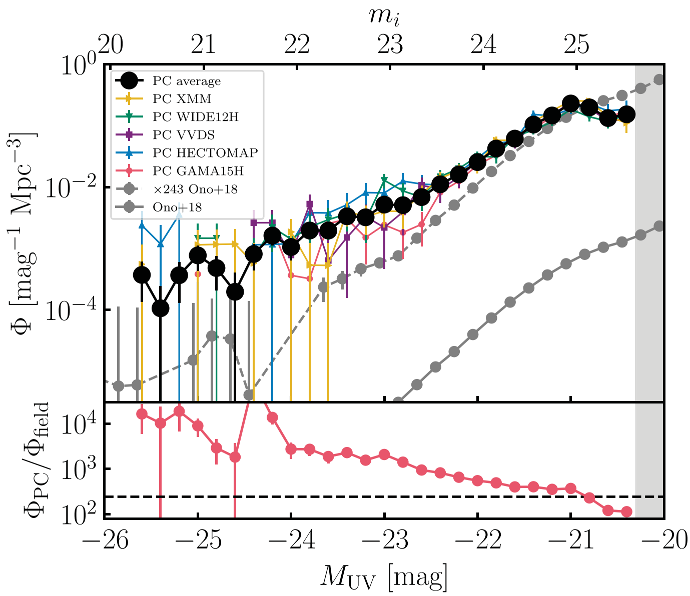

Figure 2. The UV luminosity function of galaxies in protocluster candidates at $z \sim 4$ from Ito et al. submitted. The color-coded lines represent the PC UVLF for each survey field. The black circles show the average of all fields. For reference, we show the field UVLF of Ono *et al.* (2018) (solid gray line) and shifted upward to match the PC UVLF (gray dotted line with circles). The bottom panel shows the ratio of the PC UVLF and scaled field UVLF (red circles). The black dashed line shows the value of the ratio of the sum of each UVLF. For both panels, the magnitude range that is fainter than the depth is shaded in gray.

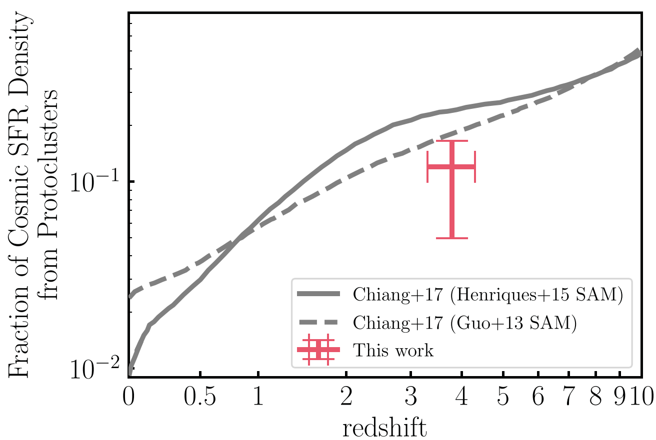

Figure 3. The fraction of the cosmic SFRD in protoclusters, edited from Ito et al. submitted. A red cross represents our estimated value for HSC-SSP protoclusters at $z \sim 4$. The gray solid and dashed lines are its predicted evolution in Chiang *et al.* (2017) with the use of the semi-analytical model of Henriques *et al.* (2015) and Guo *et al.* (2013), respectively.

The SFRD in protocluster regions can be obtained from the PC UVLF. From the PC UVLF and $\beta - M_{UV}$ relation of protocluster galaxies, we estimate the average UV luminosity density and the average FIR luminosity density via the IRX-β-M_* relation of $z \sim 3$ LBGs (Álvarez-Márquez *et al.* 2019). The UV/FIR luminosity density is converted to SFRD from the relation in Kennicut (1998). The estimated SFRD in protocluster regions

https://doi.org/10.1017/S174392132000174X Published online by Cambridge University Press

leads us to an estimate of the contribution of protocluster to the cosmic SFRD. Correcting purity and completeness of our protocluster sample, we evaluate that protoclusters contribute 5−16% of the total cosmic SFRD. This value is close to a theoretical prediction in Chiang *et al.* (2017) but slightly smaller (Figure 3). The smaller value of our result can be due to other galaxy population (e.g., sub-millimeter galaxies) in protoclusters since we only focus on g-dropout galaxies, which are typical massive star forming galaxies. Also, we define protocluster members which are located within the smallest size of protoclusters expected from simulations, which leads to an incompleteness of protocluster members. This incompleteness can also lower our estimate. On the other hand, our estimate supports that protoclusters make a non-negligible contribution to the cosmic SFRD at $z \sim 4$.

Our two studies, which focus on the UV-brightest protocluster galaxies and the PC UVLF, suggest that protocluster galaxies already have different galaxy properties even at $z \sim 4$. These galaxies are likely to have different star formation histories; they evolve earlier than other field galaxies. This evolutionary scenario is consistent with theoretical predictions (Chiang *et al.* 2017; Muldrew *et al.* 2015).

References

Aihara, H., Arimoto, N., Armstrong, R., *et al.* 2018a, *PASJ*, 70, S4
Álvarez-Márquez, J., Burgarella, D., Buat, V., *et al.* 2019, *A&A*, 630, A153
Bouwens, R. J., Illingworth, G. D., Franx, M., *et al.* 2009, *ApJ*, 705, 936
Chiang, Y.-K., Overzier, R. A., Gebhardt, K., *et al.* 2017, *ApJL*, 844, L23
Chiang, Y.-K., Overzier, R. A., & Gebhardt, K. 2013, *ApJ*, 779, 127
Cooke, E. A., Hatch, N. A., Muldrew, S. I., *et al.* 2014, *MNRAS*, 440, 3262
Dressler, A. 1980, *ApJ*, 236, 351
Guo, Q., White, S., Angulo, R. E., *et al.* 2013, *MNRAS*, 428, 1351
Hatch, N. A., Kurk, J. D., Pentericci, L., *et al.* 2011, *MNRAS*, 415, 2993
Henriques, B. M. B., White, S. D. M., Thomas, P. A., *et al.* 2015, *MNRAS*, 451, 2663
Ito, K., Kashikawa, N., Toshikawa, J., *et al.* 2019, *ApJ*, 878, 68
Kennicutt, R. C. J. 1998, *Annual Review of Astronomy and Astrophysics*, 36, 189
Koyama, Y., Kodama, T., Tadaki, K.-i., *et al.* 2013, *MNRAS*, 428, 1551
Kubo, M., Toshikawa, J., Kashikawa, N., *et al.* 2019, *ApJ*, 887, 214
Lovell, C. C., Thomas, P. A., & Wilkins, S. M. 2018, *MNRAS*, 474, 4612
Meurer, G. R., Heckman, T. M., & Calzetti, D. 1999, *ApJ*, 521, 64
Muldrew, S. I., Hatch, N. A., & Cooke, E. A. 2015, *MNRAS*, 452, 2528
Nantais, J. B., van der Burg, R. F. J., Lidman, C., *et al.* 2016, *A&A*, 592, A161
Ono, Y., Ouchi, M., Harikane, Y., *et al.* 2018, *PASJ*, 70, S10
Onoue, M., Kashikawa, N., Uchiyama, H., *et al.* 2018, *PASJ*, 70, S31
Sérsic, J. L. 1963, *Boletin de la Asociacion Argentina de Astronomia*, 6, 41
Song, M., Finkelstein, S. L., Ashby, M. L. N., *et al.* 2016,*ApJ*, 825, 5
Shibuya, T., Ouchi, M., & Harikane, Y. 2015, *ApJS*, 219, 15
Shimakawa, R., Kodama, T., Hayashi, M., *et al.* 2018, *MNRAS*, 473, 1977
Steidel, C. C., Adelberger, K. L., Shapley, A. E., *et al.* 2005, *ApJ*, 626, 44
Toshikawa, J., Uchiyama, H., Kashikawa, N., *et al.* 2018, *PASJ*, 70, S12
Uchiyama, H., Toshikawa, J., Kashikawa, N., *et al.* 2018, *PASJ*, 70, S32